

Electronic Supplementary Information (ESI)

Film Morphology of Solution-Processed Regioregular Ternary Conjugated Polymer Solar Cells under Processing Additive Stress

Jianguo Yuan,^{a,b} * Michael Ford,^b Wanli Ma^a * and Guillermo C. Bazan^b *

^aJiangsu Key Laboratory for Carbon-based Functional Materials & Devices, Institute of Functional Nano & Soft Materials (FUNSOM), Soochow University, Suzhou, Jiangsu 215123, China.

^bCenter for Polymers and Organic Solids, Departments of Chemistry and Biochemistry, University of California, Santa Barbara, CA, 93106, USA.

Email: jyyuan@suda.edu.cn (J. Yuan); [wlma@suda.edu.cn](mailto:wлма@suda.edu.cn) (W. Ma);
bazan@chem.ucsb.edu (G. C. Bazan)

Content

1. General methods
2. GIWAXS
3. DFT simulations
4. Mobility measurements by space charge limited current method
5. Solar cell performance
6. UV-vis absorption

1. General methods

Ultraviolet-Visible (UV-vis) absorption spectra were recorded on a DU-800 spectrometer. Atomic force microscopy (AFM) was conducted on an Asylum Research MFP 3D AFM, transmission electron microscopy (TEM) images were obtained using a Veeco Multimode V instrument and Tecnai T2 transmission electron microscope. 2D grazing-incidence wide-angle X-ray scattering (GIWAXS) measurements were performed at the Stanford Synchrotron Radiation Light source (SSRL) on Beamline 11-3, with a MAR345 image plate area detector, at 12.7 keV incident photon energy, and at incident angles of 0.12°. Thin film illumination occurred in a helium atmosphere to minimize X-ray beam damage.

Experimental section for EQE: EQE characteristics were measured in a nitrogen-filled glovebox using a setup consisting of a 75 W Xe light source, mono-chromator, optical chopper, lock-in amplifier, and a National Institute of Standards and Technology calibrated silicon photodiode for power-density calibration. To obtain sub-bandgap EQE, higher sensitivity settings were used with a longer time delay between measurement points. Electroluminescence spectra for the bilayers were collected directly from the solar cell devices, by applying a bias that is close to the turn-on voltage of the devices. The resulting emission was collected with a Si CCD camera cooled to -70°C. The spectra were corrected for detector response using a blackbody spectrum.

2. Grazing incidence wide angle X-ray scattering(GIWAXS)

Crystal correlation length estimates (Scherrer analysis)

The crystal correlation lengths (CCL) were estimated by the following equation:

$$CCL = \frac{2\pi}{FWHM}$$

Where FWHM is the full-width-at-half-maximum of the fitted Gaussian

Table S1. Summary of polymer and PC₇₁BM CCL values

	Processing Solvent	(100) (Z)	(010) (Z)	PCBM (Z)	(100) (XY)	PC ₇₁ BM (XY)
PSFSi F	CF	4.2 nm	4.5 nm	-	4.2 nm	-

Blend	0.0% DIO	5.6 nm	6.3 nm	2.3 nm	3.6 nm	2.7 nm
Blend	0.5% DIO	11.4 nm	6.2 nm	2.8 nm	15.1 nm	2.6 nm
Blend	2.0% DIO	12.6 nm	3.7 nm	2.3 nm	14.1 nm	2.5 nm
Blend	3.0% DIO	14.0 nm	2.7 nm	2.4 nm	14.5 nm	2.4 nm

3. DFT simulation

All quantum chemical calculations of the molecular structures were carried out based on the density functional theory (DFT) B3LYP together with 6-31G(d) basis set by using the Gaussian 09 package version C01 under the condition of tight self-consistent field convergence and ultrafine integration grids. All the alkyl chains of each molecule were replaced by methyl groups for resource-efficient calculation and clarity.

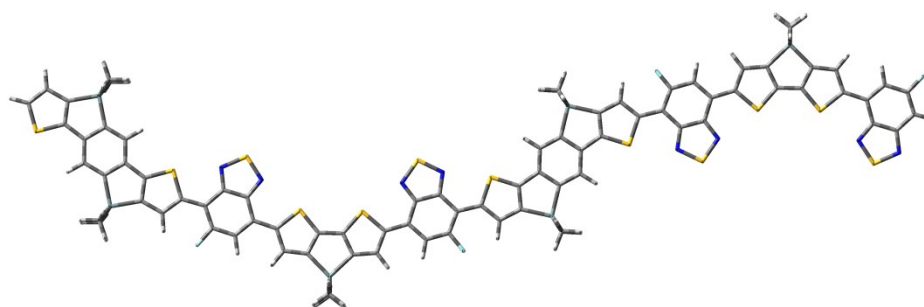


Figure S1. Optimized PIFSiF and PSFSiF dimer geometries obtained by DFT calculation.

Table S2. Summary of dihedral angles (from left to right) between each unit for all the polymers

	D1 (°)	D2 (°)	D3 (°)	D4 (°)	D5 (°)	D6 (°)	D7 (°)
PSFSiF	0.1	0.1	0.9	0.6	0.6	1.4	3.2

4. Mobility measurements by space charge limited current method

Hole-only and electron-only devices were fabricated to measure the hole and electron mobility using the space charge limited current (SCLC) method. The hole-only device structure is ITO/PEDOT:PSS/polymer or blend/Au (50 nm) and the electron-only device structure is ITO/ZnO/polymer or blend/LiF (0.6 nm) /Al (80 nm). The thickness was measured by Profilometer. The mobility was determined by fitting the dark current to the model of a single carrier SCLC, which is described by the equation:

$$J = \frac{9}{8} \epsilon_0 \epsilon_r \mu_h \frac{V^2}{d^3},$$

Where J is the current, ϵ_0 is the permittivity of free space, ϵ_r is the relative permittivity of the material, μ is the zero-field mobility, d is the thickness of the polymer layer, V is the applied voltage. Then hole mobilities were calculated from the fitting slope of the $J^{1/2}$ - V curves below (V_{bi} was selected 0.4 V for neat polymer and 0.45 V for polymer-fullerene blend when performing SCLC fit):

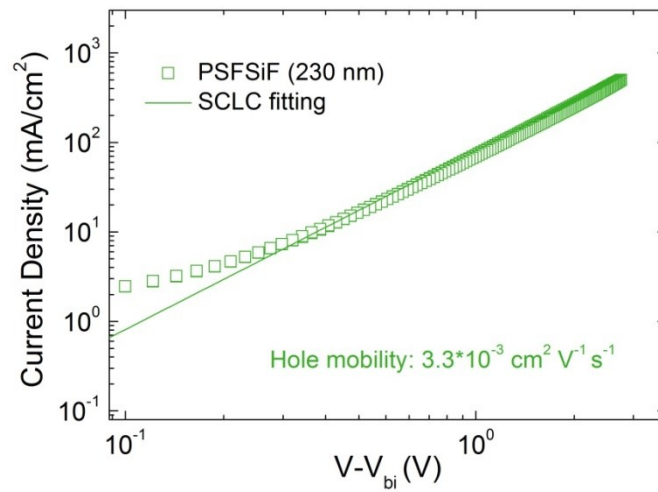


Figure S2. J - V curves of neat polymer hole-only diodes devices.

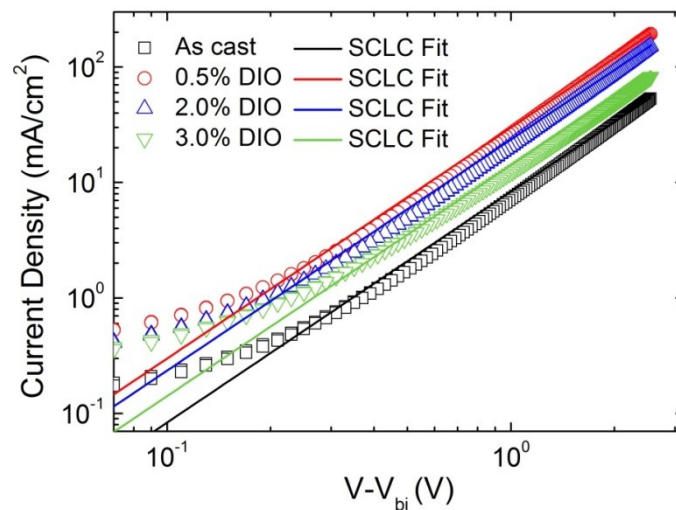


Figure S3. J - V curves of hole-only diodes devices based on PSFSiF blend with varying DIO content.

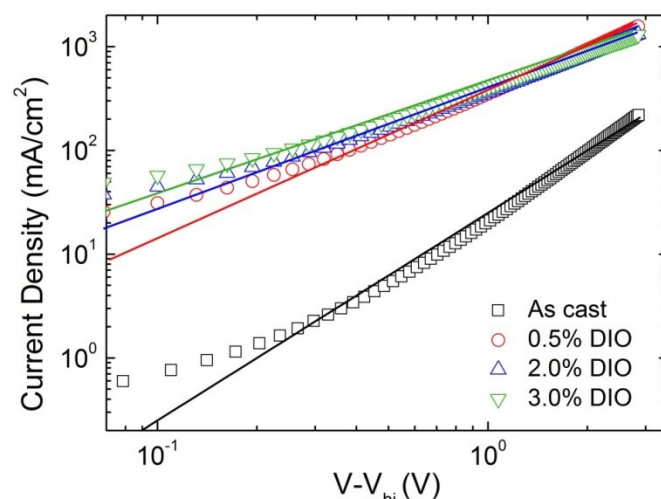


Figure S4. J - V curves of electron-only diodes devices based on PSFSiF blend with varying DIO content.

Table S3. SCLC hole and electron mobility of PSFSiF/PC₇₁BM cast from chloroform with different DIO content

Film	As cast	0.5% DIO	2.0% DIO	3.0% DIO
Thickness (nm)	100	105	110	120
Fit Slope(hole)	8.34	32.98	22.50	14.12
SCLC hole mobility (cm ² V ⁻¹ s ⁻¹)	2.8*10 ⁻⁵	1.3*10 ⁻⁴	9.0*10 ⁻⁵	5.7*10 ⁻⁵
Fit Slope(Electron)	20.91	185.78	180.40	175.6
SCLC electron mobility (cm ² V ⁻¹ s ⁻¹)	7.0*10 ⁻⁵	7.3*10 ⁻⁴	7.2*10 ⁻⁴	7.1*10 ⁻⁴

5. Solar Cells Performance

Device Fabrication: Solution-processed solar cells devices were fabricated with a conventional architecture of ITO/PEDOT:PSS/active layer/Ca/Al, an inverted structure of ITO/ZnO/active layer/MoO_x/Ag, respectively. The ITO-coated glass substrates were firstly cleaned by ultrasonic treatment in detergent, deionized water, acetone and isopropyl alcohol for 30 minutes each, and subsequently dried in an oven overnight. After treated with UV/ozone for 30 min, PEDOT:PSS (Al 4083) layer was deposited and dried at 150 °C in ambient atmosphere for 10 mins. Active layers were spun at varying spin rate from PSFSiF:PC₇₁BM solutions at different weight ratios, cathodes were

deposited by sequential thermal evaporation of 10 nm of calcium followed by 80 nm of aluminum. The device area was 4.5 mm².

Device Characterization : Photovoltaic characterization was performed on a Keithley 2602 source measure unit with a 300 W Xe arc lamp and an AM 1.5 global filter. The solar simulator illumination intensity was measured using a KG1 filter from the National Renewable Energy Laboratory (NREL) with a silicon photovoltaic.

Table S4. Performance of PSFSiF under the conventional structure using different solvents. (ITO/PEDOT:PSS/PSFSiF:PC₇₁BM (1:1, w/w)/Ca/Al, each condition average result is based on five devices. CF: chloroform; CB: chlorobenzene; ODCB: *o*-dichlorobenzene, TA: thermal annealing at 120 °C for 10 min)

Solvent.	V _{oc} (V)	J _{sc} (mA/cm ²)	FF	PCE (%) Average	PCE (%) Best
CF	0.80	7.52	0.40	2.30	2.43
CF+TA	0.80	5.64	0.34	1.41	1.53
CF+0.5% DIO	0.74	16.66	0.58	6.98	7.10
CF+2.0% DIO	0.70	16.26	0.46	5.08	5.22
CB	0.82	6.93	0.44	2.30	2.47
CB+TA	0.82	7.27	0.45	2.51	2.65
CB+0.5% DIO	0.74	12.91	0.49	4.51	4.64
CB+2.0% DIO	0.74	14.35	0.47	4.84	5.00
ODCB	0.82	10.86	0.51	4.45	4.54
ODCB+TA	0.80	12.54	0.52	5.07	5.24
ODCB+0.5% DIO	0.76	13.39	0.53	5.13	5.38
ODCB+2.0% DIO	0.74	11.38	0.51	4.13	4.30

Table S5. Performance of ITO/PEDOT:PSS/PSFSiF:PC₇₁BM/Ca/Al in different D/A ratio. (Each condition average result is based on five devices.)

D/A ratio	V _{oc} (V)	J _{sc} (mA/cm ²)	FF	PCE (%) Average	PCE (%) Best
1:1+0.5% DIO	0.74	16.63	0.60	7.23	7.40
1:1.5+0.5% DIO	0.72	15.99	0.62	7.04	7.14
1:1.5+1.0% DIO	0.72	15.20	0.53	5.49	5.78
1:2 0.5% DIO	0.72	15.53	0.59	6.37	6.56

1:2 1.0% DIO	0.70	15.96	0.47	5.06	5.21
1:2 2.0% DIO	0.70	15.62	0.45	4.73	4.90

Table S6. Performance of ITO/PEDOT:PSS(PH)/PSFSiF:PC71BM (1:1 w/w, CF+0.5% DIO)/Ca/Al in different thickness. (Each condition average result is based on five devices, devices in vacuum overnight before Ca and Al were evaporated)

Spin rate (rpm)	Thickness (nm)	V_{oc} (V)	J_{sc} (mA/cm ²)	FF (%)	PCE (%) Average	PCE (%) Best
800	220	0.72	14.95	0.52	5.38	5.55
1200	140	0.74	16.18	0.56	6.52	6.67
1500	115	0.74	16.29	0.63	7.29	7.55
1750	105	0.74	17.02	0.63	7.62	7.99
2000	96	0.74	15.77	0.62	6.98	7.22
2500	84	0.74	15.58	0.60	6.59	6.88

Table S7. Optimized device performance based on PSFSiF with different DIO additive content. (ITO/PEDOT:PSS/PSFSiF:PC₇₁BM/Ca/Al)

DIO (%)	V_{oc} (V)	J_{sc} (mA/cm ²)	FF	PCE (%) Average	PCE (%) Best
PSFSiF 0.0	0.80	7.52	0.40	2.30	2.43
PSFSiF 0.5	0.74	17.02	0.63	7.62	8.00
PSFSiF 1.0	0.74	16.65	0.61	7.20	7.45
PSFSiF 2.0	0.72	16.60	0.55	6.27	6.53
PSFSiF 3.0	0.72	15.69	0.49	5.26	5.55

Table S8. 10 devices performance based on ITO/PEDOT:PSS (PH)/ PSFSiF:PC71BM (1:1 w/w, CF+0.5% DIO)/Ca/Al with best condition

Device No.	V_{oc} (V)	J_{sc} (mA/cm ²)	FF	PCE (%)
1	0.74	16.66	0.60	7.45
2	0.74	17.57	0.61	7.90
3	0.74	16.25	0.61	7.35
4	0.74	15.99	0.63	7.46
5	0.74	16.28	0.63	7.56
6	0.74	16.64	0.61	7.51
7	0.74	16.10	0.62	7.42
8	0.74	16.12	0.64	7.65

9	0.74	17.02	0.63	8.00
10	0.74	16.85	0.62	7.76
Average	0.74	16.55	0.62	7.62

6. UV-vis absorption

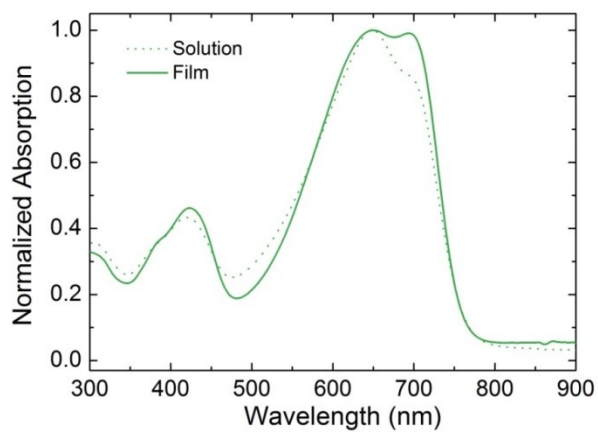


Figure S5. Solution and thin film UV-vis absorption of regioregular ternary polymer PSFSiF.

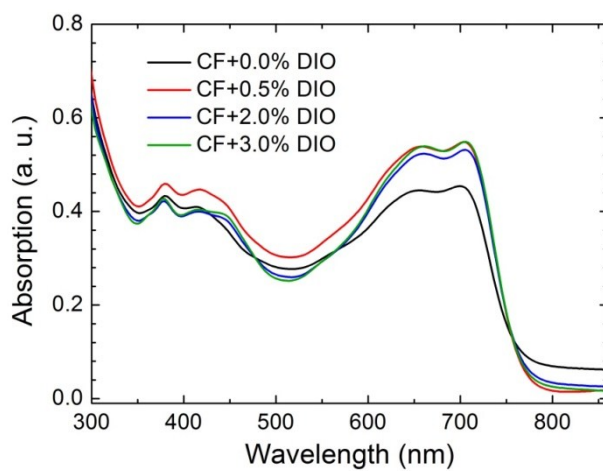


Figure S6. UV-vis absorption of PSFSiF/PC₇₁BM blends with varying DIO content.